Characterisation of PGs1, a subunit of a protein complex co-purifying with tubulin polyglutamylase

Catherine Regnard[2,*], Didier Fesquet[1], Carsten Janke[1], Dominique Boucher[2], Elisabeth Desbruyères[2], Annette Koulakoff[3], Christine Insina[1], Pierre Travo[1] and Bernard Eddé[1,‡]

[1]Centre de Recherches de Biochimie Macromoléculaire, CNRS, 34293 Montpellier, France
[2]Laboratoire de Biochimie Cellulaire, CNRS, Université Paris 6, 75252 Paris, France
[3]INSERM U114, Collège de France, 75005 Paris, France
*Present address: Department of Molecular Biology, Adolf Butenandt Institute, 80336 Munich, Germany
‡Author for correspondence (e-mail: edde@crbm.cnrs-mop.fr)

Accepted 4 July 2003
Journal of Cell Science 116, 4181-4190 © 2003 The Company of Biologists Ltd
doi:10.1242/jcs.00743

Summary

Polyglutamylation is a post-translational modification initially discovered on tubulin. It has been implicated in multiple microtubule functions, including neuronal differentiation, axonemal beating and stability of the centrioles, and shown to modulate the interaction between tubulin and microtubule associated proteins. The enzymes catalysing this modification are not yet known. Starting with a partially purified fraction of mouse brain tubulin polyglutamylase, monoclonal antibodies were raised and used to further purify the enzyme by immunoprecipitation. The purified enzyme complex (M_r 360×10^3) displayed at least three major polypeptides of 32, 50 and 80×10^3, present in stochiometric amounts. We show that the 32×10^3 subunit is encoded by the mouse gene *GTRGEO22*, the mutation of which has recently been implicated in multiple defects in mice, including male sterility. We demonstrate that this subunit, called PGs1, has no catalytic activity on its own, but is implicated in the localisation of the enzyme at major sites of polyglutamylation, i.e. neurones, axonemes and centrioles.

Supplemental data available online

Key words: Axoneme, Cell cycle, Centrosome, Neurone, Polyglutamylation, Tubulin

Introduction

Microtubules (MTs) play fundamental roles in multiple cellular processes (Hyams and Lloyd, 1993) and there is a growing list of factors and molecular motors that regulate the organisation and the spatiotemporal remodelling of the MT network (Drewes et al., 1998; Kobayashi and Mundel, 1998; McIntosh et al., 2002).

Tubulin the protein that constitutes MTs is highly heterogeneous, especially in the C-terminal tail, which is important for the binding of most microtubule-associated proteins (MAPs). Each of the two subunits (α and β) is encoded by a multigene family of 6-8 members in mammals. In addition to this genetic diversity, seven different types of post-translational modifications have been evidenced so far, which further increases the heterogeneity of the protein (Luduena, 1998). This heterogeneity is thought to allow MTs to undergo specialised functions, as formulated a number of years ago in 'the multi-tubulin hypothesis' (Fulton and Simpson, 1976). In the last few decades, numerous observations have supported this hypothesis (Edde et al., 1987; Edde et al., 1983; Gard and Kirschner, 1985; Kreitzer et al., 1999) even though there are many more hallmarks of tubulin heterogeneity with mysterious functions.

Among tubulin modifications, polyglutamylation (Edde et al., 1990) and polyglycylation (Redeker et al., 1994) are very unusual post-translational modifications, consisting of the sequential addition of glutamate and glycine units, respectively. The first added unit is linked by an isopeptidic bond to the γ-carboxyl of a glutamate residue of the main polypeptidic chain. Addition of the other units occurs through classic peptide bonds and leads to the formation of polyglutamyl or polyglycyl chains of various lengths. Interestingly, polyglutamylation is not restricted to tubulin, it was recently shown to occur on nucleosome assembly proteins NAP1 and NAP2 (Regnard et al., 2000), nucleoplasmin (our unpublished results), and probably on several yet unidentified proteins.

Polyglutamylation of tubulin is a widespread modification prevailing in centrioles (Bobinnec et al., 1998b), basal bodies and axonemes (Fouquet et al., 1994; Gagnon et al., 1996). In neurones, most of the tubulin is polyglutamylated (Audebert et al., 1994) whereas it is present, albeit at low levels in most, if not all, non-neuronal cells and tissues analysed (Wolff et al., 1994; Regnard et al., 1999; Kann et al., 2003).

An increasing amount of data strongly suggests a major role for polyglutamylation in regulating MT functions. Indeed, masking of the polyglutamyl side chain with a specific monoclonal antibody (GT335) was shown to strongly inhibit axonemal beating (Gagnon et al., 1996; Million et al., 1999) and led to the disappearance of centrioles and the dispersion of the pericentriolar material in cells (Bobinnec et al., 1998a). In addition, the extent of the modification seems to have a fine tuning effect since the in vitro binding of various MAPs and

MT motors are influenced by the length of the polyglutamyl side chain (Bonnet et al., 2001; Boucher et al., 1994; Larcher et al., 1996).

To better understand the function of polyglutamylation, identification of polyglutamylase(s) is a crucial step. We believe that mouse brain tubulin polyglutamylase (TPG) is a multimeric complex composed of at least three different polypeptides of M_r 32, 50 and 80×10^3 and we describe the function of the 32×10^3 subunit, called PGs1, as an addressing subunit for a subset of polyglutamylases, including neuronal, centriolar and axonemal TPGs.

Materials and Methods

Plasmids and protein expression

Mouse PGs1 cDNA was PCR amplified from mouse brain cDNA and cloned into pET15b (Novagen) and into pEGFP-N1 (Clonetech). PGs1 was expressed in *E. coli* BL21 DE3. Inclusion bodies were obtained from the pellet of the crude cell extract by several washing steps in 10 mM Tris-HCl, pH 7.5, 1 M NaCl, 10 mM EDTA, 5% Triton X-100. PGs1 accounted for >90% of the proteins of the inclusion bodies.

ΔmPGs1 was amplified from the vector pEGFP-mPGs1 in two steps: (1) amplification of the 5′ fragment (1-165) with a 5′ primer and a fusion primer (bridging the deletion); (2) amplification of the 3′ part of ΔmPGs1 (255-912) with the PCR-product of step 1 and a 3′ primer. The PCR-product of step 2 was exchanged with mPGs1 in pEGFP-mPGs1 to obtain pEGFP-ΔmPGs1 (Δ166-254). Sequencing and western blot analysis revealed the expression of the correct mutant protein.

Northern blot

Northern mouse tissue blot (from V. Coulon, IGM, Montpellier, France) was hybridised with radio-labelled PGs1 cDNA as described by De Toledo et al. (De Toledo et al., 2001).

Antibodies

Monoclonal antibodies (mAbs) against a 400× purified fraction of TPG [fraction IV (Regnard et al., 1998)] were generated by injecting 50 μg into 8-week-old BALB/c mice. Cell fusion with mouse myeloma cells P3-X63-Ag8.653 was carried out (de StGroth and Scheidegger, 1980). Out of 322 hybridomas, 11 positive clones, characterised by the ability to deplete TPG activity, were obtained. mAb206 (IgG2a, κ) was affinity purified on a Sepharose-Protein G column (Amersham Pharmacia Biotech) from ascite fluid from clone 206 (Eurogentec, Belgium).

Polyclonal antibody L83 was raised in rabbit against PGs1 inclusion bodies and purified by affinity chromatography on PGs1 linked to CNBr-activated Sepharose (Amersham Pharmacia Biotech). The specificity of L83 was confirmed by western blot analysis.

Other antibodies used in this study were mAb GT335 (Wolff et al., 1994), mAb anti-γ-tubulin (GTU-88; Sigma), mAb anti-α-tubulin (DM1A; Amersham Pharmacia Biotech), mAbs anti-RIIα and -RIIβ of PKA (Transduction Laboratories). Anti-centrosome mAb (CTR453) was a gift from Dr G. Keryer (Institut Curie, Paris, France). Its epitope was recently mapped to centrosomal AKAP450 (Keryer et al., 2003).

TPG assay

Tubulin polyglutamylase activity was measured by the incorporation of L-[^{3}H]glutamate (45-55 Ci/mmol; Amersham, UK) into taxotere-stabilised MTs, as described previously (Regnard et al., 1998).

Purification and identification of mouse brain TPG

A TPG fraction IV was obtained from 150 3-day-old mouse brains as described by Regnard et al. (Regnard et al., 1998), and concentrated by ammonium sulfate precipitation at 40% saturation. All steps were performed at 4°C. The pellet was solubilised in TBSTx (50 mM Tris-HCl, pH 7.6, 100 mM NaCl, 0.1% Triton X-100), containing protease inhibitors, cleared by centrifugation, and pre-incubated with protein G magnetic beads (Dynal Biotech) bound to mouse non-specific Igs (Sigma). The supernatant was incubated overnight with 100 μl bead suspension bound to affinity-purified mAb206. The beads were extensively washed with TBSTx; 0.5 M NaCl, and bound proteins were resolved on a 10% SDS gel and stained with Coomassie Blue (Serva). Protein bands were excised and digested with trypsin (Seq. grade; Promega).

Mass spectrometry

Aliquots of analytes solutions (0.7 μl) were mixed with the same volume of alpha-cyano-4-hydroxy-*trans*-cinnamic acid as matrix (10 mg/ml in 50% acetonitrile, 0.1% trifluoroacetic acid) and loaded onto the probe. Analysis was performed using a Biflex III MALDI-TOF mass spectrometer (Bruker-Franzen Analytik, Bremen, Germany) in reflectron mode. The accelerating voltage was 20 kV with a delayed extraction of 400 nseconds. Spectra were analysed using XTOF software (Bruker-Franzen Analytik). Autoproteolysis products of trypsin (Ms: 842.51, 1045.56, 2211.10) were used as internal calibrates. The p32 protein was identified by Mascot search (www.matrixscience.com).

Electrophoresis and western blotting

1D-PAGE was performed according to the method of Laemmli, (Laemmli, 1970). Protein concentration was determined with Bradford reagent (Sigma). Affinity-purified L83 was diluted at 0.2 μg/ml and donkey anti-rabbit Ig (Amersham Pharmacia Biotech) 1:10,000 in PBSTw (PBS; 0.1% Tween 20). Blots were developed with Western Lightning Chemo-luminescence Reagent Plus (NEN).

Cell culture and transfection

Multipotential embryonal carcinoma cell line PCC7-AzaR1 1009 (Pfeiffer et al., 1981), here denoted 1009, was obtained from the Pasteur Institute (Paris, France). Cells were grown in DME medium (Invitrogen) containing 15% foetal calf serum. Cells blocked in mitosis were collected after an 11-hour incubation with 1 μM nocodazole (Sigma). Cell transfection was carried out at 30% confluence using Lipofectamine Plus reagent (Invitrogen). Stable transfected 1009 cells were selected through several passages in culture medium containing 0.8 mg/ml geneticin (Invitrogen).

Neurones were isolated from foetal mouse brains at 15 days of gestation and allowed to develop in culture, as described previously (Berwald-Netter et al., 1981). Neural cells depleted in neurones were cultured as described previously (Alvarez-Buylla et al., 2001).

Light microscopy

1009 cells were cultured on glass coverslips under standard culture conditions and fixed either with 3.7% paraformaldehyde at room temperature, for 15 minutes or with methanol at –20°C, for 8 minutes and incubated with L83 (2 μg/ml), GT335 (5 μg/ml), GTU-88 (1:500), CTR453 (1:10), DM1A (1:1000) or anti-RIIα and β (1:150) for 1 hour, followed by 30 minutes with either donkey anti-rabbit Ig, Texas Red-conjugated (Amersham Pharmacia Biotech; 1:200), or Rhodamine- or Fluoresceine-conjugated goat anti-mouse Ig (Jackson ImmunoResearch Laboratories; 1:200). Coverslips were mounted with Vectashield mounting medium (Vector Laboratories).

Microscopes used were DMIRBO or DMRA microscopes (Leica, Germany). For confocal microscopy, a DMRA microscope was equipped with a module Ultraview (Perkin Elmer, UK). Imaging software used was Metamorph (Universal Imaging Copp., USA). For deconvolution and 3-D reconstruction, image stacks were processed on a SGI octane workstation running Huygens (Scientific Volume Imaging b.v., Netherlands) using MLE algorithms. 3-D restored stacks were processed with Imaris 3 (Bitplane, Switzerland) for volume rendering. Live cells were observed with a DM IRBE inverted microscope with a PL APO 63× oil immersion objective.

Results

Purification of brain TPG

We have previously reported a 1000-fold purification of tubulin polyglutamylase from 3-day-old mouse brain. This partially purified fraction still contained a number of protein species, preventing the identification of the enzyme (Regnard et al., 1998). We thus decided to develop an alternative strategy and produced monoclonal antibodies against the 400× purified fraction of TPG. These antibodies were selected for their capacity to immuno-precipitate the enzymatic activity from brain TPG fractions.

Antibodies from each hybridoma were bound to a mixture of protein A and protein G and incubated with fraction II [a 20× purified fraction (Regnard et al., 1998)]. TPG activity was then measured in the supernatant and bead fraction (Fig. 1, upper and lower panels, respectively). Of the 330 tested hybridomas, 11 were able to deplete TPG, albeit with variable efficiency (30-90% depletion). In each instance, both α- and β-TPG activities were depleted to the same extent (β:α ratio, 1:3). TPG activity was recovered in the bead fractions but with a low yield, presumably because the beads hinder proper interaction of the bound enzyme with the large MT substrates. None of the selected hybridomas produced antibodies able to significantly inhibit TPG activity in vitro or to detect protein by western blot analysis.

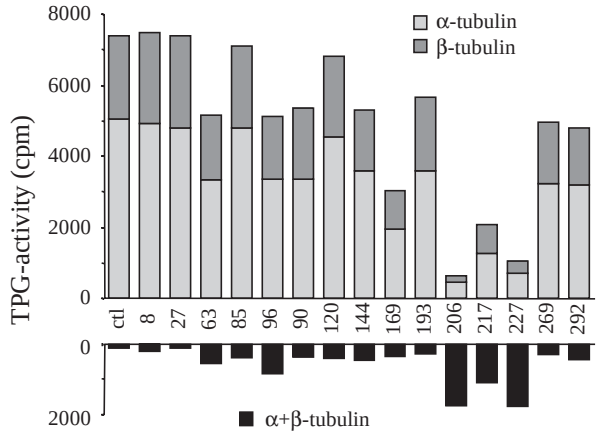

Fig. 1. Screening of anti-TPG hybridomas. Of the 330 hybridomas tested, 15 are presented here. TPG activity was measured in both the supernatant (top) and bead fraction (bottom) of each IP. Incorporation of [^{3}H]Glu into α-tubulin (light-grey bars) and β-tubulin (dark-grey bars) was measured separately for the supernatants and together for the pellets (black bars). The control (Ctl) is an IP performed with the culture medium alone. Numbering refers to hybridoma names.

As mAb206 has the best efficiency, it was used for further purification of TPG by immunoprecipitation of fraction IV (Fig. 2A). Apart from the antibody heavy (HC) and light (LC)

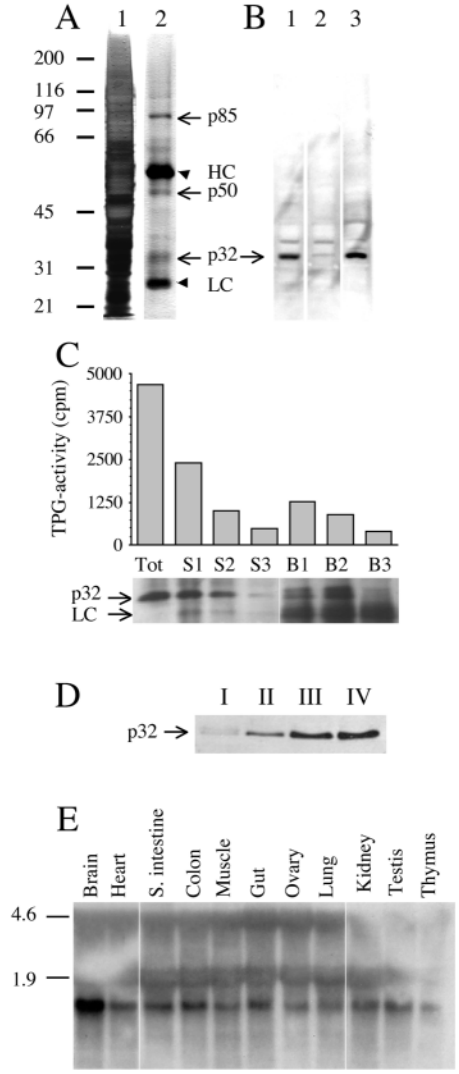

Fig. 2. Immunoprecipitation of brain TPG and identification of the PGs1 subunit. (A) Silver staining of Fraction IV (lane 1) and the IP fraction obtained with mAb206 (lane 2). In addition to the light (LC) and heavy (HC) antibody chains (arrowheads), three protein species (arrows) are found at high levels in the IP fraction. (B) Immunoprecipitation was performed with mAb206 and analysed by western blotting with L83. Comparable amounts of fraction IV (lane 1), unbound fraction (lane 2) and IP fraction (lane 3) were loaded on the gel. (C) L83 immunoprecipitates TPG activity. S1-S3 correspond to the IP supernatants obtained after the first, second and third cycle of IP, and B1-B3 to the bead fractions. Similar proportions of each fraction were tested for TPG activity (upper panel) and analysed by western blotting with L83 (lower panel). The position of p32 and of the antibody light chain are indicated by arrows. (D) Enrichment of PGs1 during TPG purification. Brain fractions I (initial supernatant) and II-IV [20×, 160× and 400× purified fractions, respectively, as described by Regnard et al. (Regnard et al., 1998)] were analysed by western blotting with L83. Equal amounts of proteins were loaded in each lane. (E) PGs1 mRNA expression profile. Total RNA from various mouse tissues were analysed by northern blotting and probed with a ^{32}P-labelled PGs1 cDNA ORF.

chains, three prominent protein species at M_r 32, 50 and 80×10^3 were detected in the immunoprecipitate by silver staining of the gel (Fig. 2A). Thus, TPG appears to be a multimeric complex. A dimer of the three proteins would give a total mass of 324×10^3, which is in good agreement with the previously measured mass (360×10^3) of the enzyme in native conditions (Regnard et al., 1998).

Identification of PGs1

Tryptic digests from each protein in the gel were analysed by mass spectrometry. Database searches identified the 32×10^3 protein as the product of a mouse gene called *GTRGEO22* (in Mascot search, this was the only sequence which gave a significant probability based mowse score, 93). This gene is composed of two small exons separated by a large intron and is located on chromosome 10 (accession number, AF303106). It encodes a 303 amino acid protein (M_r 32.6×10^3, pI 8.95) of unknown function, containing a putative A-kinase-anchoring protein (AKAP) binding domain in the first exon (ProtFam accession number: PF02297). The protein is conserved in human (locus 19p13.3) and other vertebrates as well as in the invertebrate *Ciona intestinalis* (see Supplementary Fig. 1: http://jsc.biologists.org/supplemental) but no clear orthologues were found in plants, *Drosophila* or *Caenorhabditis*.

We cloned the cDNA corresponding to the mouse *GTRGEO22* gene and raised polyclonal antibodies against bacterially expressed recombinant protein. Affinity-purified antibodies (hereafter denoted L83) specifically reacted with the recombinant protein (data not shown) and with the protein species of 32×10^3 in fraction IV (Fig. 2B, lane 1). The p32 protein is efficiently immunoprecipitated with mAb206 (Fig. 2B, lanes 2 and 3) along with 90% of TPG activity. Likewise, L83 immunoprecipitates both p32 protein and TPG activity. When three consecutive cycles of immunoprecipitation are performed, ~90% of TPG activity is depleted and recovered in the consecutive bead fractions (Fig. 2C). To further confirm that p32 is genuinely part of the TPG complex, the different fractions obtained during the purification procedure were analysed by western blotting with L83. As shown in Fig. 2D, a very faint signal was detected in the starting brain fraction (fraction I). This signal increased strongly in parallel with the extent of TPG purification (fractions II-IV) [see Regnard et al. (Regnard et al., 1998) for a description of the different fractions]. Therefore, the p32 protein is subsequently called PGs1 for polyglutamylase subunit 1.

Expression pattern of PGs1

Western blot analysis of PGs1 in a number of cell and tissue extracts did not yield detectable signals (data not shown), except in brain (Fig. 2D). However, northern blot analysis on various mouse tissues shows that PGs1 mRNA is present at low levels in most adult tissues tested, and at a significantly higher level in brain (Fig. 2E). These results correlate with the abundance of polyglutamylated tubulin as well as with the distribution of TPG activity, which is higher in extracts from brain and neurones than in other tissues and cell lines (Regnard et al., 1998; Regnard et al., 1999; Wolff et al., 1994).

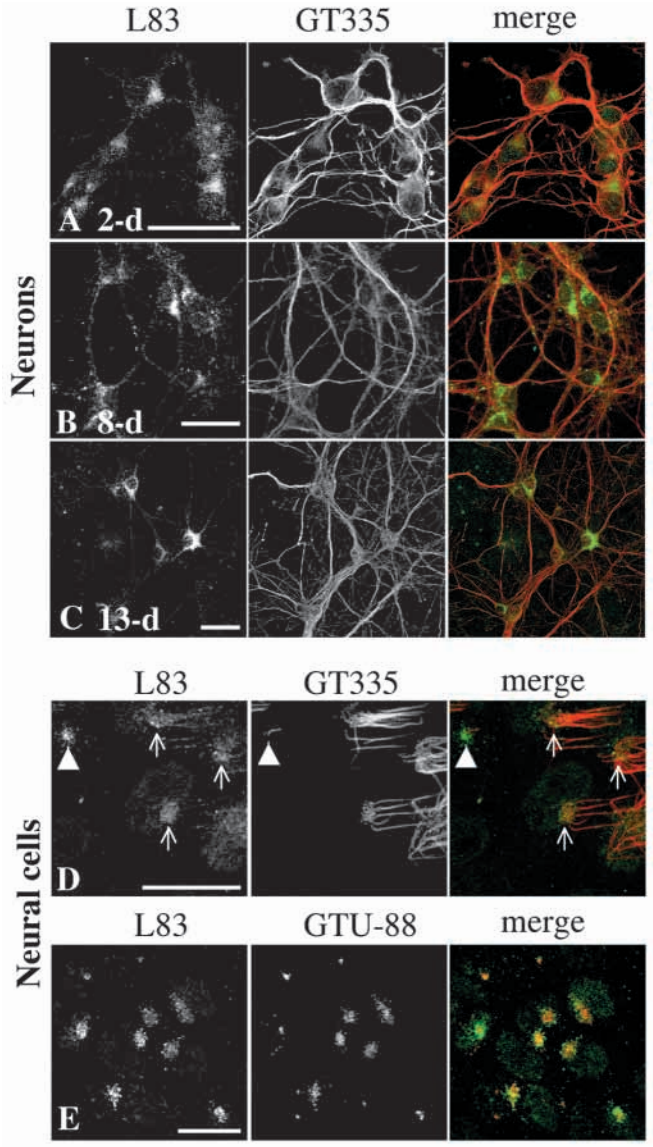

Fig. 3. Confocal images of PGs1 localisation in mouse neural cells in primary culture. (A-C) Mouse brain neurones were cultured for 2 (A), 8 (B) and 13 (C) days, then fixed with paraformaldehyde and double stained with L83 (left panels, green) and GT335 (middle panels, red). Right panels present the corresponding merged images. (D,E), Mouse brain neural cells fixed with paraformaldehyde and double stained with L83 (left panels in D and E, green) and GT335 (middle panel in D, red) or anti-γ-tubulin mAb GTU-88 (middle panel in E, red). Right panels show the corresponding merged images. Staining of PGs1 was observed at the base of primary cilia (arrowheads) as well as of multiple cilia emerging from ependymal cells (arrows). Note also some PGs1 staining along the cilia. Scale bars: 20 μm.

PGs1 is associated with major sites of tubulin polyglutamylation

We next analysed the subcellular distribution of PGs1 by immunofluorescence on primary cultures of neurones from embryonic mouse cortex. In young neurones, after 2 days in culture, L83 stains several dots in the cell soma, which are more concentrated in the region where neurites emerge (Fig.

3A). In more differentiated neurones, after 8 to 13 days in culture (Fig. 3B,C), a stronger punctuate labelling is detected both in the cell somata and in the proximal part of the neurites. Double staining of the neurones with L83 and GT335, a mAb raised against the polyglutamylated motif (Wolff et al., 1994) showed a restricted co-localisation. The majority of PGs1 is in the proximal part of neurites whereas only some dot-like structures localise along the entire length of neurites, which contain the strongly polyglutamylated microtubules (Fig. 3A-C).

To determine whether PGs1 is a neurone-specific subunit of TPG or is shared by other polyglutamylases, we analysed its distribution in other cell types. Ciliated and flagellated cells are of particular interest since axonemes contain strongly polyglutamylated tubulins (Fouquet et al., 1994; Gagnon et al., 1996; Million et al., 1999). Mixed neural cell cultures depleted in neurones contain, in addition to astrocytes, ependymal cells characterised by the presence of multiple cilia and cells that exhibit a single cilium (Alvarez-Buylla et al., 2001). In the latter, L83 decorates the base of the cilium (Fig. 3D, arrowhead). Similar but stronger staining is observed at the base of multiple cilia emerging from ependymal cells (Fig. 3D, arrows). Some dots are also observed along the length of cilia indicating a partial co-localisation of PGs1 with the strongly polyglutamylated MTs of axonemes. Double labelling with L83 and anti-γ-tubulin antibodies reveal an overlap of PGs1 and γ-tubulin in all cells present in the culture, suggesting that PGs1 is also present at the centrosomes (Fig. 3E). Finally, in mouse spermatozoa, a strong concentration of PGs1 in the proximal part of the flagella is observed (data not shown).

Taken together, these results show that PGs1 is enriched in the vicinity of major sites of tubulin polyglutamylation, i.e. neurites, centrosomes, basal bodies and axonemes. There is, however, no strict co-localisation of PGs1 and polyglutamylated tubulin since the strongly glutamylated MTs in neurites and ciliary axonemes are poorly labelled with L83.

PGs1 is addressing TPG to the centrosome in exponentially growing cells

In exponentially growing cells the overall polyglutamylation of tubulin is low and restricted to the β-tubulin subunit, except for the highly modified centriolar MTs, which are mostly glutamylated on the α-tubulin subunit (Bobinnec et al., 1998b). To better examine the association of PGs1 with the centrosome we used the mouse teratocarcinoma cell line 1009, which can be grown as multipotential embryonal carcinoma (EC) cells or induced to differentiate into neurone-like cells (Edde et al., 1983; Lang et al., 1989). In EC cells, PGs1 is detected as a punctuate stain focusing in one region of the cell (Fig. 4). Co-labelling with GT335, GTU-88 (anti-γ-tubulin) and CTR-453 (anti-AKAP450) shows that PGs1 staining includes the centrioles and overlaps with γ-tubulin and AKAP450 staining (Fig. 4).

Centrosomal localisation of PGs1 is further confirmed by transient expression of PGs1-GFP in 1009 EC cells. Labelling with L83 shows a complete co-localisation with the green fluorescence indicating the specificity of our antibody as well as the correct localisation of the overexpressed and tagged protein (Fig. 5A). In all transfected cells, PGs1-GFP accumulates around the centrosome, as evidenced by labelling

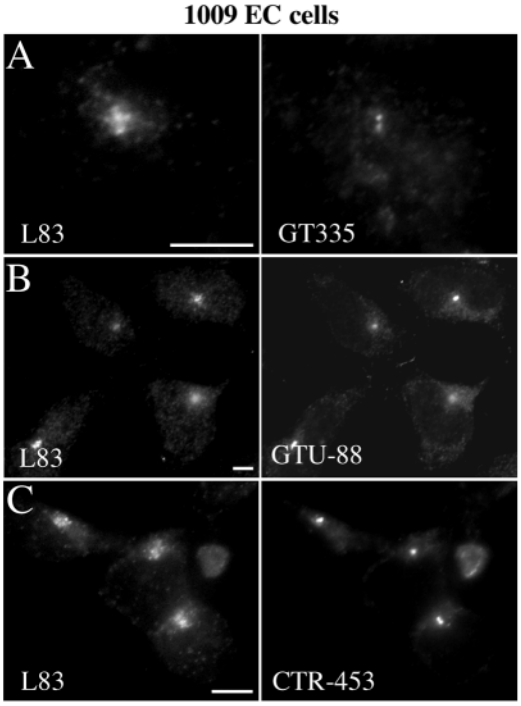

Fig. 4. PGs1 is localised at the centrosome in 1009 EC cells. Exponentially growing 1009 EC cells were fixed with methanol and double stained with L83 (left panels) and anti-polyglutamylated tubulin (GT335, right panel in A) or anti-γ-tubulin (GTU-88, right panel in B), or anti-AKAP450 (CTR-453, right panel in C). Scale bars: 10 μm.

with mAb CTR-453 (Fig. 5B). Control cells transfected with GFP alone present a diffuse staining in the whole cytoplasm (not shown).

Stable cell lines expressing PGs1-GFP were established. The GFP-tagged protein has the proper localisation at the centrosome both in paraformaldehyde-fixed cells (Fig. 5C) and in unfixed cells (Fig. 5D). Western blotting with L83 shows that only PGs1-GFP (~60×10^3) is detected in total cell extracts suggesting that the tagged protein is at least in a 10-fold excess compare to the endogenous PGs1 (Fig. 5E). Thus, the mechanism enabling PGs1-GFP localisation at the centrosome is not saturated. In addition, neither the GT335 reactivity nor the TPG activity is significantly increased in those cells (not shown), suggesting that PGs1 has no glutamylation activity on its own. This subunit is most probably implicated in intracellular addressing of the TPG protein complex.

The putative AKAP binding domain of PGs1 has no role in centrosomal localisation

PGs1 contains a sequence that exhibits homology to the AKAP-binding domain of cAMP-dependent protein kinase (PKA; Supplementary Fig. 1: http://jsc.biologists.org/supplemental). This domain is found in the RII subunits of PKA and has been shown to be implicated in targeting the kinase at specific subcellular sites, one of which is the centrosome, through interaction with AKAPs (for reviews, see Colledge and Scott, 1999; Diviani and Scott, 2001). We examined the role of this

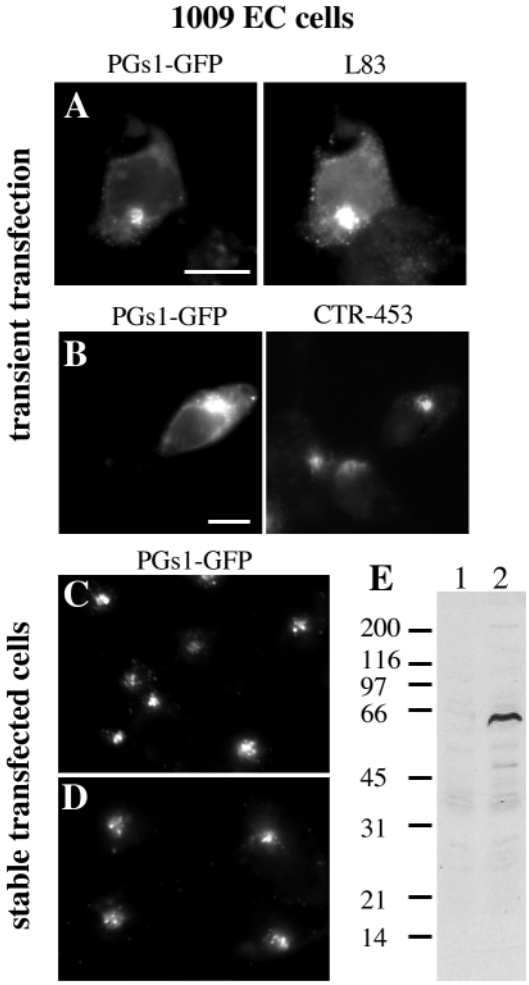

Fig. 5. PGs1-GFP localises to the centrosome. (A,B) 1009 cells were transfected with a PGs1-GFP construct and analysed 24 hours after transfection. Cells were fixed with paraformaldehyde and stained with L83 (right panel in A) or CTR-453 (right panel in B). Left panels show PGs1-GFP fluorescence. (C,D), PGs1-GFP fluorescence of stable transfected 1009 cells, fixed with paraformaldehyde (C) or unfixed (D). Scale bars: 10 μm. (E) Western blotting of 1009 (lane 1) and stable transfected 1009/PGs1-GFP (lane 2) cell extracts with L83. A single band at 60×10^3 was detected in the latter but not in the former. Note that the endogenous PGs1 is not detected.

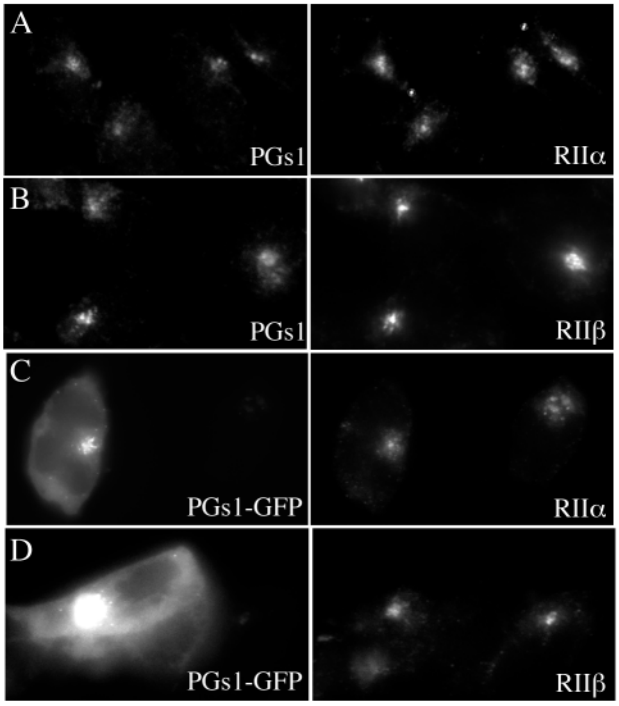

Fig. 6. PGs1 co-localises with PKA. (A,B) Exponentially growing 1009 EC cells were fixed with methanol and double stained with L83 (left panels) and anti-RIIα (right panel in A) or anti-RIIβ (right panel in B). (C,D) 1009 cells were transfected with a PGs1-GFP construct and analysed 24 hours after transfection. Cells were fixed with paraformaldehyde and stained with anti-RIIα (right panel in C) or anti-RIIβ (right panel in D). Left panels show PGs1-GFP fluorescence. Scale bars: 10 μm.

sequence in PGs1 targeting. Double staining of PGs1 with either the RIIα or RIIβ subunit of PKA shows co-localisation of both proteins at the centrosome (Fig. 6A,B), raising the possibility that PGs1 could be targeted to the centrosome by the same mechanism as PKA. However, overexpression of PGs1-GFP in 1009 cells does not modify the centrosomal localisation of PKA, indicating that PGs1 and PKA do not compete with each other for the same sites on the centrosome (Fig. 6C,D). In addition, an overexpressed ΔPGs1-GFP mutant protein that is missing the putative AKAP-binding motive (amino acids 56-85), localises at the centrosome in a manner indistinguishable from that of the wild-type PGs1-GFP fusion protein (not shown). These results indicate that localisation of PGs1 at the centrosome does not involve the putative AKAP binding domain of the protein.

Three-dimensional organisation of PGs1 on the centrosome

To better define the centrosomal area where the endogenous PGs1 is localised we analysed co-staining images of PGs1 with polyglutamylated tubulin (Fig. 7A), γ-tubulin (Fig. 7B) and AKAP-450 (Fig. 7C) by deconvolution and 3-D reconstruction. L83 staining (red) does not overlap with GT335 staining (green) of the centrioles, but builds an additional layer surrounding the γ-tubulin and AKAP450 clouds (green) (Fig. 7A-C). Co-staining with anti-α-tubulin mAb (green, Fig. 7D) showed that MTs extend within this layer and revealed, in addition, that smaller dots of PGs1 present in the cytoplasm are located in the close vicinity of MTs to which they seem to be associated. These observations culminate with the suggestion that PGs1 is concentrated around the centrosome, but not directly anchored to this structure.

Centrosomal localisation of PGs1 is dependent on the integrity of the MT network

To test if MTs are implicated in the centrosomal localisation of PGs1, we studied the localisation of PGs1 in cells treated with drugs affecting the polymerisation state of MTs. Incubation of 1009 EC cells with 10 μM nocodazole for 45 minutes leads to the depolymerisation of almost all MTs and is accompanied by the diffusion of PGs1 into the

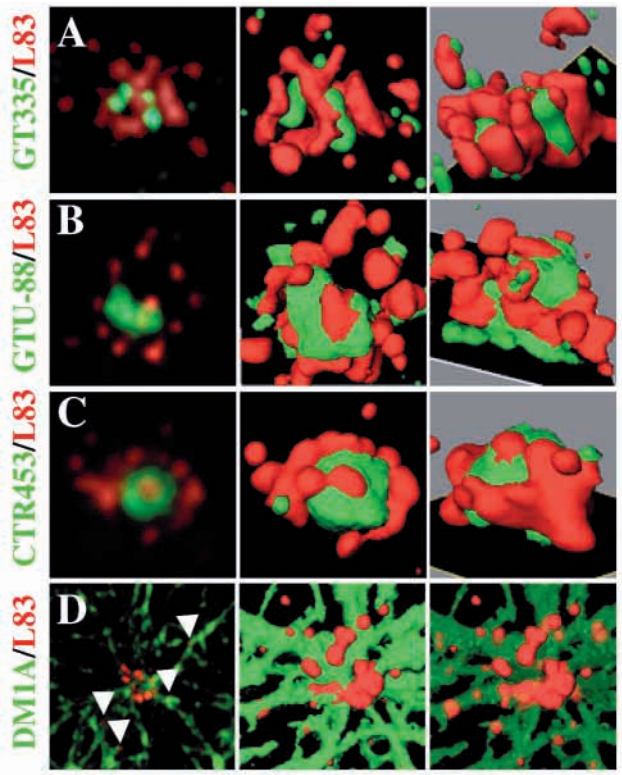

Fig. 7. 3D reconstruction of PGs1 at the centrosome. 1009 EC cells were fixed with methanol and double stained with L83 (red) and GT335 (A, green) or GTU-88 (B, green) or CTR-453 (C, green) or DM1A (D, green). Confocal images were analysed by deconvolution. Projections of all planes are shown in left panels. 3D reconstructions are shown in the middle and right panels in two different orientations. In D (right), the green colour was made semi-transparent to better visualise the red staining. The arrowheads in D (left), indicate PGs1 dots associated with MTs.

cytoplasm (Fig. 8A,B). Washing off nocodazole results in a rapid re-growth of MTs from the centrosomes and a redistribution of PGs1. 3 minutes after washing, PGs1 is detected along the length of the newly nucleated microtubules (Fig. 8C) and begins to concentrate at the centre of the aster. 3 minutes later, PGs1 is almost entirely focused at the centre of the microtubule network (Fig. 8D). Similar results were obtained with live 1009/PGs1-GFP cells (Fig. 8F-H). Delocalisation of PGs1 is also observed when cells are treated with 5 μM taxol for 45 minutes, but as expected in this case, PGs1 is found associated with the MT bundles (Fig. 8E). From these observations we conclude that PGs1 is not directly anchored at the centrosome, but transported towards, and maintained at, the centrosome via its association with the MT network.

Localisation of PGs1 is regulated during the cell cycle

In the 1009 EC cell line, endogenous PGs1 is found at the centrosome in the majority of the cells in interphase but is hardly detectable in mitotic cells (not shown). Fig. 9A,B show similar results obtained from fixed 1009EC/PGs1-GFP cells. These observations were confirmed by time-lapse imaging. A

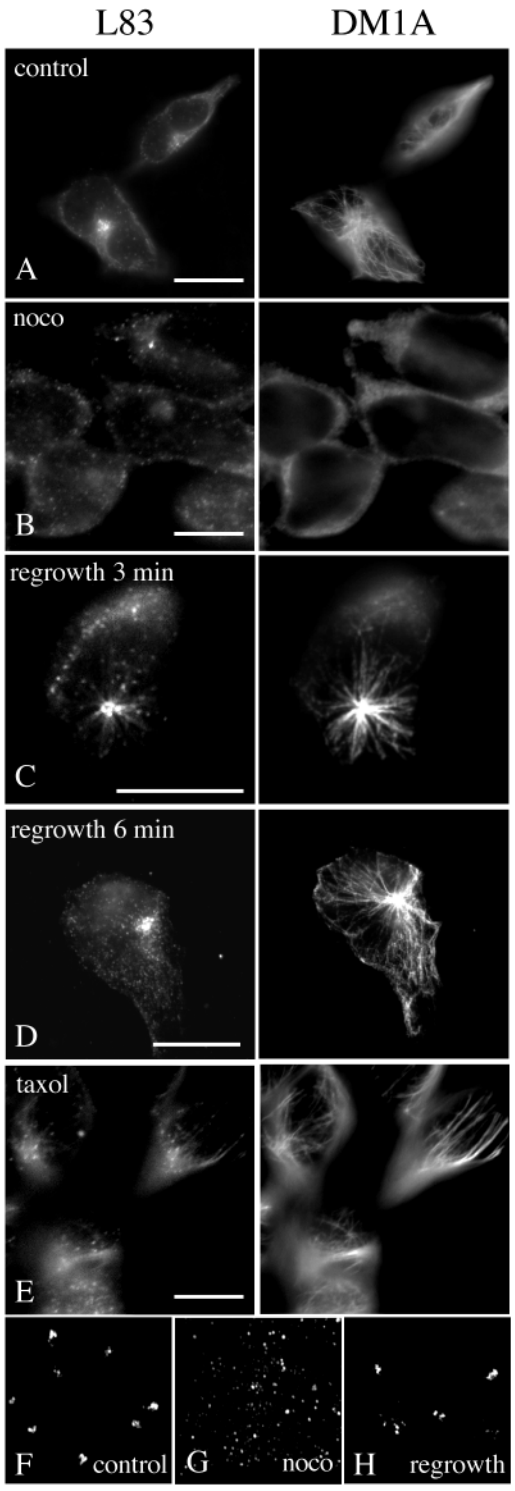

Fig. 8. Localisation of PGs1 is dependent on the integrity of the MT network. 1009 cells were incubated with (B) or without (A) 10 μM nocodazole for 45 minutes. After washing off nocodazole, MTs were allowed to regrow for 3 minutes (C) or 6 minutes (D). (E) 1009 cells were incubated with 5 μM taxol for 45 minutes. Methanol-fixed cells were double stained with L83 (left panels in A-E) and DM1A (right panels in A-E). Scale bars: 10 μm. (F-H) Confocal green fluorescence images of living 1009/PGs1-GFP cells before (F) and after incubation with 10 μM nocodazole for 45 minutes (G) and after 10 minutes of regrowth (H).

typical example, presented in Fig. 9C, shows a cell going through mitosis. The green label remains focused for 30 minutes and then becomes suddenly faint and diffuse at 40 minutes, when chromosomes appear nicely aligned on the metaphase plate. These data indicate that de-localisation of PGs1 occurs at the G2-M transition. As cells exit mitosis (70 minutes), PGs1-GFP is again detectable and focused, indicating that after cytokinesis, the protein is rapidly recruited again to the centrosomes. These observations show that localisation of PGs1 to the centrosome is cell-cycle regulated.

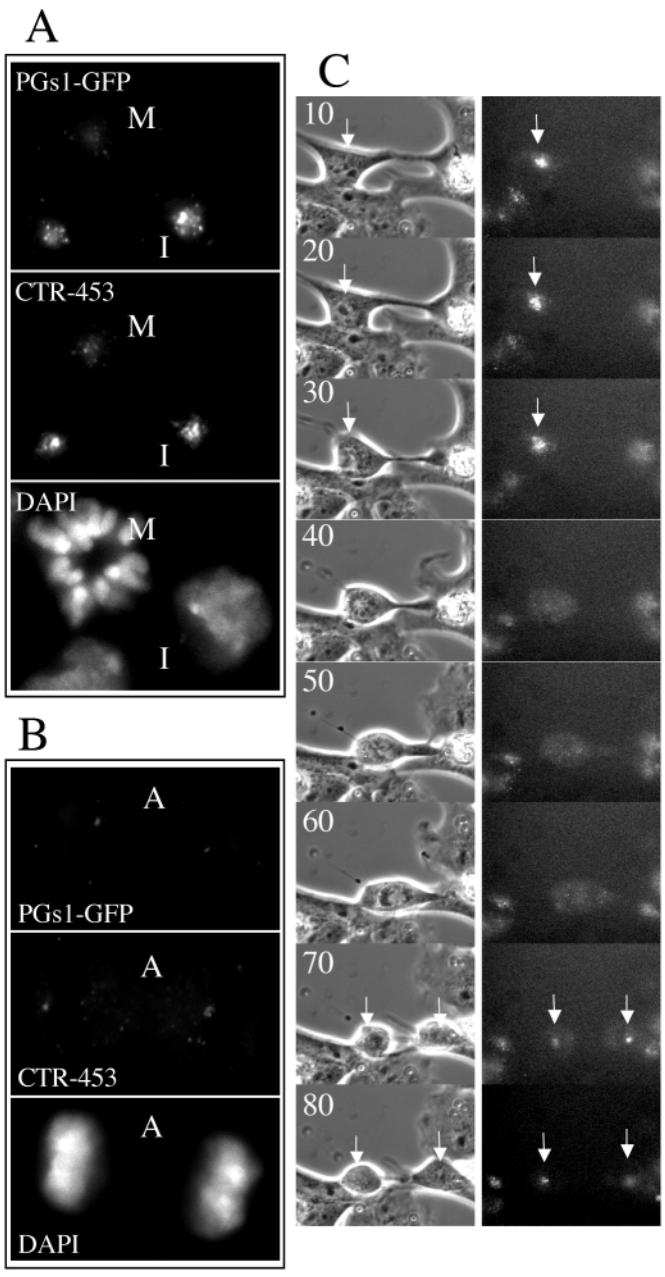

Fig. 9. PGs1 disappears from centrosomes at mitosis. (A,B) Fixed 1009/PGs1-GFP cells immunolabelled with CTR-453 (middle panels). Upper panels show the green fluorescence of PGs1-GFP and lower panels DAPI staining of DNA. The intensity of labelled cells in interphase (I), metaphase (M) and anaphase (A) is compared. (C) Time-lapse video microscopy of 1009/PGs1-GFP cells. Phase contrast (left panels) and green fluorescence (right panels) images were taken at 10 minutes intervals. Arrows indicate a cell that goes through mitosis during the time course of the experiment.

Discussion

TPG is a multimeric enzyme

In this report, we present evidence that mammalian brain tubulin polyglutamylase is a complex of at least three major protein species. These proteins seem to be present in stoechiometric amounts, indicating that the enzyme complex is likely composed of two molecules of each subunit. Such a complex would have a total mass of approximately 324×10^3) close to the value of 360×10^3 determined from the sedimentation coefficient (10 S) and Rs (70 Å) in native conditions (Regnard et al., 1998). We describe here the 32×10^3 subunit of the complex, called PGs1, in more detail. The two other proteins co-purifying with PGs1, p50 and p80, were recently identified as proteins of yet unknown function for which a detailed analysis is going on in the laboratory.

PGs1 was identified as the product of the gene *GTRGEO22* in mouse, initially annotated as encoding for a putative protein of unknown function. Several lot of data strongly argue for considering PGs1 as a subunit of TPG. First, antibodies raised against PGs1 (L83) immunoprecipitate TPG activity. Conversely, a monoclonal antibody, selected for its capacity to immunoprecipitate TPG activity, immunoprecipitates PGs1. Second, PGs1 is enriched during the purification of TPG in a manner similar to that of TPG activity. Third, PGs1 is concentrated around known major sites of tubulin polyglutamylation, namely MTs in neurones, centrosomes, basal bodies and axonemes. In addition, a recent report shows that an insertional mutation localised in *GTRGEO22* results in pleiotropic effects, including complete male sterility due to strong defects in sperm flagella development (Campbell et al., 2002). Identification of PGs1 as the polypeptide encoded by this gene strongly argues for a direct role of polyglutamylation in the morphogenesis of the complex MT assembly of axonemes. This conclusion is strengthened by previous data showing that polyglutamylation is actually implicated in axoneme beating (Gagnon et al., 1996; Million et al., 1999) and in the stability of centrioles (Bobinnec et al., 1998a).

Recently, TPG from *Crithidia* was proposed to be a NIMA-related protein, called CfNek (Westermann and Weber, 2002). As its most closely related mammalian Nek2 orthologue (Fry et al., 1995), CfNek exhibits a β-casein kinase activity. The authors proposed that polyglutamylation could require the phosphotransferase activity of this protein to generate peptidic bonds. We found that some α- and β-casein kinase activities are present in fraction IV, but were lost after TPG pull down (data not shown), suggesting that brain TPG does not contain a Nek-related subunit and could follow a different catalytic mechanism. Mammalian and *Crithidia* TPGs differ also by their overall organisation, since the latter has been purified as a single polypeptide displaying a sedimentation coefficient of 3S (Westermann et al., 1999). Such strong differences are rather unexpected but could be related to the more complex functions of polyglutamylation in multi-cellular organisms, compared to flagellates. Nevertheless, it is interesting to note

that CfNek is associated with basal bodies in *Crithidia* (Westermann and Weber, 2002) and Nek2 with centrosomes in higher eukaryotes (Fry et al., 1998), raising the possibility that the latter kinase could be implicated in the regulation of some aspects of polyglutamylation.

PGs1 localisation and the mechanism of MT polyglutamylation

Overexpression of PGs1 in cultured cells does not lead to any detectable increase in TPG activity. In particular, no increase of the polyglutamylation levels of centrosomes and cytoplasmic microtubules was observed by IF labelling with GT335. In addition, when cell extracts of 1009/PGs1-GFP were assayed for in vitro polyglutamylation, no increase over control non transfected cells was observed. These data suggest that one or both of the other subunits of the complex are required for TPG activity and are likely limiting in transfected cells. Thus PGs1 has no catalytic activity on its own. The localisation data presented here favour a role of PGs1 in addressing TPG at particular sites of polyglutamylation.

In neurones, PGs1 is mostly found in the cell body and in the proximal part of the neuronal processes whereas polyglutamylated tubulin is highly enriched all along neurites. This suggests that MTs or tubulin oligomers are polyglutamylated before or just upon their entry into the neurites. At the centrosome, PGs1 is found in close proximity, but not directly in contact, with the strongly polyglutamylated centriolar MTs. Again, this pattern favours a model of polyglutamylation of tubulin occurring before its incorporation into the centriole. In addition, as PGs1 localises at the base of cilia and in the proximal part of flagella, polyglutamylation most likely occurs before the transport of tubulin to the tip of the axonemes where it will be incorporated in the axonemal structure (Iomini et al., 2001).

However, cytoplasmic MTs nucleating at the centrosome or present in the vicinity of the base of cilia are not or very poorly polyglutamylated (Bobinnec et al., 1998b; Million et al., 1999; Kann et al., 2003). One explanation would be the presence of a strong deglutamylation activity selectively present in the cytoplasm, which would counterbalance TPG activity. Alternatively, we cannot exclude, at present, that the TPG complex is localised around centrosomes and basal bodies as a kind of stock pile, from which the core enzyme could dissociate to selectively interact and polyglutamylate those structures.

PGs1 is addressed at the centrosome in a cell cycle-dependent way

In 1009 cells overexpressing PGs1-GFP the majority of the protein is detected at the centrosome, in a manner indistinguishable from the endogenous protein. Since the levels of PGs1-GFP greatly exceed that of the endogenous protein, the centrosomal localisation of PGs1 is probably independent of the presence of the other TPG subunits which would be titered out. However, unlike other centrosomal proteins such as pericentrin and γ-tubulin (Young et al., 2000), PGs1 is completely delocalised upon disruption of the MT network, suggesting that the protein is not anchored at the centrosome. During MT re-growth, PGs1 rapidly associates with the newly nucleated MTs and accumulates in the pericentriolar area. This suggests that PGs1 is transported along MTs by a minus-end-directed motor activity. 3-D reconstruction of PGs1/tubulin double staining strongly suggests that, although PGs1 forms a complex matrix surrounding the centrioles, most elements of this matrix directly interact with the minus end regions of centrosomal MTs. It is thus likely that both the transport and the association of PGs1 with centrosomes are directly and exclusively dependent on the interaction with MTs. The dissociation of PGs1 from centrosomes observed in mitosis could then be due to the depolymerisation of the interphasic MT network. Preliminary experiments performed on nocodazole-arrested mitotic 1009/PGs1-GFP cells, suggest that partial degradation of PGs1 might also occur at the time of mitosis and could prevent re-association with the mitotic spindle and poles. However, an additional mechanism avoiding re-association with MTs is likely to be implicated, since the residual non-degraded PGs1-GFP present in these cells diffuses in the cytoplasm and does not localise either on the spindles or at the spindle poles.

It is important to note that PGs1 contains a domain located in the N-terminal part of the protein (aa 56-85) which shows homology to a consensus sequence from regulatory subunits of PKA. This sequence was shown to be responsible for the dimerisation of PKA and binding of PKA to AKAPs (for reviews, see Colledge and Scott, 1999; Diviani and Scott, 2001). Our data show that PGs1 follows a particular pathway for centrosomal localisation, which does not involve the putative AKAP binding domain. Whether this domain plays other functions remains to be investigated.

PGs1 and isozymic variants of TPG.

The question of how the different substrates (α-tubulin, β-tubulin and NAPs) could be specifically polyglutamylated is a central issue. Brain TPG is not active on NAP substrate (our unpublished results). It was shown to preferentially polyglutamulate α-tubulin, but polyglutamylation of the β-subunit also occurs, albeit at a much lower rate (β:α ratio, 1:3) (Regnard et al., 1998). In contrast, the major activity present in HeLa cells strongly polyglutamylates β-tubulin and NAPs, but not α-tubulin. It is interesting to note that a minor activity is also present in these cells, with a strong specificity towards α-tubulin and is indistinguishable from the brain TPG. This minor type is solubilised only at high salt concentration, suggesting that it is associated with a rather insoluble structure, possibly centrosomes (Regnard et al., 1999). We thus propose the existence of two main polyglutamylase types. Type I would be the main type present in proliferative cells and responsible for the polyglutamylation of β-tubulin and probably NAPs. Type II would be responsible for the preferential activity towards α-tubulin observed in neurones, axonemes and centrioles. The molecular composition of type I polyglutamylase is at present not known. It is likely that specific domains or subunits of the polyglutamylase complex could be involved in substrate specificity and localisation sites. The data presented here suggest that PGs1 is specific to type II polyglutamylase and functions as a localisation subunit.

We gratefully acknowledge the technical contributions of N. Camcho and C. Pellet. We also thank P. Huitorel for immunolabelling of spermatozoa, G. Keryer for providing polyclonal and monoclonal (CTR-453) anti-AKAP450 antibodies, A. Fry for providing Nek2

recombinant protein and anti-Nek2 antibodies, J. Derancourt and E. Demey for mass spectrometry analysis, J. C. Larcher, P. Steffen and P. Chaussepied for helpful discussion. This work was supported by the Association de la Recherche Contre le Cancer (ARC 5859 to B.E. and ARC 5479 to D.F.) and EMBO Long-term Fellowship (ALTF 387-2001 to C.J.).

References

Alvarez-Buylla, A., Garcia-Verdugo, J. M. and Tramontin, A. D. (2001). A unified hypothesis on the lineage of neural stem cells. *Nat. Rev. Neurosci*. **2**, 287-293.

Audebert, S., Koulakoff, A., Berwald-Netter, Y., Gros, F., Denoulet, P. and Edde, B. (1994). Developmental regulation of polyglutamylated alpha- and beta-tubulin in mouse brain neurons. *J. Cell Sci*. **107**, 2313-2322.

Berwald-Netter, Y., Martin-Moutot, N., Koulakoff, A. and Couraud, F. (1981). Na+-channel-associated scorpion toxin receptor sites as probes for neuronal evolution in vivo and in vitro. *Proc. Natl. Acad. Sci. USA* **78**, 1245-1249.

Bobinnec, Y., Khodjakov, A., Mir, L. M., Rieder, C. L., Edde, B. and Bornens, M. (1998a). Centriole disassembly in vivo and its effect on centrosome structure and function in vertebrate cells. *J. Cell Biol*. **143**, 1575-1589.

Bobinnec, Y., Moudjou, M., Fouquet, J. P., Desbruyeres, E., Edde, B. and Bornens, M. (1998b). Glutamylation of centriole and cytoplasmic tubulin in proliferating non-neuronal cells. *Cell. Motil. Cytoskeleton* **39**, 223-232.

Bonnet, C., Boucher, D., Lazereg, S., Pedrotti, B., Islam, K., Denoulet, P. and Larcher, J. C. (2001). Differential Binding Regulation of Microtubule-associated Proteins MAP1A, MAP1B, and MAP2 by Tubulin Polyglutamylation. *J. Biol. Chem*. **276**, 12839-12848.

Boucher, D., Larcher, J. C., Gros, F. and Denoulet, P. (1994). Polyglutamylation of tubulin as a progressive regulator of in vitro interactions between the microtubule-associated protein Tau and tubulin. *Biochemistry* **33**, 12471-12477.

Campbell, P. K., Waymire, K. G., Heier, R. L., Sharer, C., Day, D. E., Reimann, H., Jaje, J. M., Friedrich, G. A., Burmeister, M., Bartness, T. J. et al. (2002). Mutation of a novel gene results in abnormal development of spermatid flagella, loss of intermale aggression and reduced body fat in mice. *Genetics* **162**, 307-320.

Colledge, M. and Scott, J. D. (1999). AKAPs: from structure to function. *Trends Cell. Biol*. **9**, 216-221.

de StGroth, S. F. and Scheidegger, D. (1980). Production of monoclonal antibodies: strategy and tactics. *J. Immunol. Methods* **35**, 1-21.

De Toledo, M., Coulon, V., Schmidt, S., Fort, P. and Blangy, A. (2001). The gene for a new brain specific RhoA exchange factor maps to the highly unstable chromosomal region 1p36.2-1p36.3. *Oncogene* **20**, 7307-7317.

Diviani, D. and Scott, J. D. (2001). AKAP signaling complexes at the cytoskeleton. *J. Cell Sci*. **114**, 1431-1437.

Drewes, G., Ebneth, A. and Mandelkow, E. M. (1998). MAPs, MARKs and microtubule dynamics. *Trends Biochem. Sci*. **23**, 307-311.

Edde, B., de Nechaud, B., Denoulet, P. and Gros, F. (1987). Control of isotubulin expression during neuronal differentiation of mouse neuroblastoma and teratocarcinoma cell lines [published erratum appears in *Dev. Biol.* (1988) **126**, 215]. *Dev. Biol*. **123**, 549-558.

Edde, B., Jakob, H. and Darmon, M. (1983). Two specific markers for neural differentiation of embryonal carcinoma cells. *EMBO J*. **2**, 1473-1478.

Edde, B., Rossier, J., Le Caer, J. P., Desbruyeres, E., Gros, F. and Denoulet, P. (1990). Posttranslational glutamylation of alpha-tubulin. *Science* **247**, 83-85.

Fouquet, J. P., Edde, B., Kann, M. L., Wolff, A., Desbruyeres, E. and Denoulet, P. (1994). Differential distribution of glutamylated tubulin during spermatogenesis in mammalian testis. *Cell Motil. Cytoskeleton* **27**, 49-58.

Fry, A. M., Meraldi, P. and Nigg, E. A. (1998). A centrosomal function for the human Nek2 protein kinase, a member of the NIMA family of cell cycle regulators. *EMBO J*. **17**, 470-481.

Fry, A. M., Schultz, S. J., Bartek, J. and Nigg, E. A. (1995). Substrate specificity and cell cycle regulation of the Nek2 protein kinase, a potential human homolog of the mitotic regulator NIMA of Aspergillus nidulans. *J. Biol. Chem*. **270**, 12899-12905.

Fulton, C. and Simpson, P. (1976). Selective synthesis and utilization of flagelar tubulin. The multitubulin hypothesis. In *Cell Motility* (ed. R. Goldman, T. Pollard and J. L. Rosenbaum), pp. 987-1005. Cold Spring Harbor, New York: Cold Spring Harbor Laboratory.

Gagnon, C., White, D., Cosson, J., Huitorel, P., Edde, B., Desbruyeres, E., Paturle-Lafanechere, L., Multigner, L., Job, D. and Cibert, C. (1996). The polyglutamylated lateral chain of alpha-tubulin plays a key role in flagellar motility. *J. Cell Sci*. **109**, 1545-1553.

Gard, D. L. and Kirschner, M. W. (1985). A polymer-dependent increase in phosphorylation of beta-tubulin accompanies differentiation of a mouse neuroblastoma cell line. *J. Cell Biol*. **100**, 764-774.

Hyams, J. S. and Lloyd, C. W. (1993). *Microtubules*. Wiley-Liss, New York.

Iomini, C., Babaev-Khaimov, V., Sassaroli, M. and Piperno, G. (2001). Protein particles in Chlamydomonas flagella undergo a transport cycle consisting of four phases. *J. Cell Biol*. **153**, 13-24.

Kann, M.-L., Soues, S., Levilliers, N. and Fouquet, J.-P. (2003). Glutamylated tubulin: Diversity of expression and distribution of isoforms. *Cell. Motil. Cytoskeleton* **55**, 14-25.

Keryer, G., Witczak, O., Delouvée, A., Kemmner, W. A. Rouillard, D., Taskén, K. and Bornens, M. (2003). Dissociating the centrosomal matrix protein AKAP450 from centrioles impairs centriole duplication and cell cycle progression. *Mol. Biol. Cell* **14**, 2436-2446.

Kobayashi, N. and Mundel, P. (1998). A role of microtubules during the formation of cell processes in neuronal and non-neuronal cells. *Cell Tissue Res*. **291**, 163-174.

Kreitzer, G., Liao, G. and Gundersen, G. G. (1999). Detyrosination of tubulin regulates the interaction of intermediate filaments with microtubules in vivo via a kinesin-dependent mechanism. *Mol. Biol. Cell* **10**, 1105-1118.

Laemmli, U. K. (1970). Cleavage of structural proteins during the assembly of the head of bacteriophage T4. *Nature* **227**, 680-685.

Lang, E., Mazauric-Stuker, M. L. and Maelicke, A. (1989). States of developmental commitment of a mouse embryonal carcinoma cell line differentiating along a neural pathway. *J. Cell Biol*. **109**, 2481-2493.

Larcher, J. C., Boucher, D., Lazereg, S., Gros, F. and Denoulet, P. (1996). Interaction of kinesin motor domains with alpha- and beta-tubulin subunits at a tau-independent binding site. Regulation by polyglutamylation. *J. Biol. Chem*. **271**, 22117-22124.

Luduena, R. F. (1998). Multiple forms of tubulin: different gene products and covalent modifications. *Int. Rev. Cytol*. **178**, 207-275.

McIntosh, J. R., Grishchuk, E. L. and West, R. R. (2002). Chromosome-microtubule interactions during mitosis. *Annu. Rev. Cell Dev. Biol*. **18**, 193-219.

Million, K., Larcher, J., Laoukili, J., Bourguignon, D., Marano, F. and Tournier, F. (1999). Polyglutamylation and polyglycylation of alpha- and beta-tubulins during in vitro ciliated cell differentiation of human respiratory epithelial cells. *J. Cell Sci*. **112**, 4357-4366.

Pfeiffer, S. E., Jakob, H., Mikoshiba, K., Dubois, P., Guenet, J. L., Nicolas, J. F., Gaillard, J., Chevance, G. and Jacob, F. (1981). Differentiation of a teratocarcinoma line: preferential development of cholinergic neurons. *J. Cell Biol*. **88**, 57-66.

Redeker, V., Levilliers, N., Schmitter, J. M., Le Caer, J. P., Rossier, J., Adoutte, A. and Bre, M. H. (1994). Polyglycylation of tubulin: a posttranslational modification in axonemal microtubules. *Science* **266**, 1688-1691.

Regnard, C., Audebert, S., Desbruyeres, E., Denoulet, P. and Edde, B. (1998). Tubulin polyglutamylase: partial purification and enzymatic properties. *Biochemistry* **37**, 8395-8404.

Regnard, C., Desbruyeres, E., Denoulet, P. and Edde, B. (1999). Tubulin polyglutamylase: isozymic variants and regulation during the cell cycle in HeLa cells. *J. Cell Sci*. **112**, 4281-4289.

Regnard, C., Desbruyeres, E., Huet, J. C., Beauvallet, C., Pernollet, J. C. and Edde, B. (2000). Polyglutamylation of nucleosome assembly proteins. *J. Biol. Chem*. **275**, 15969-15976.

Westermann, S. and Weber, K. (2002). Identification of CfNek, a novel member of the NIMA family of cell cycle regulators, as a polypeptide copurifying with tubulin polyglutamylation activity in Crithidia. *J. Cell Sci*. **115**, 5003-5012.

Westermann, S., Schneider, A., Horn, E. K. and Weber, K. (1999). Isolation of tubulin polyglutamylase from Crithidia; binding to microtubules and tubulin, and glutamylation of mammalian brain alpha- and beta-tubulins. *J. Cell Sci.* **112**, 2185-2193.

Wolff, A., Houdayer, M., Chillet, D., de Nechaud, B. and Denoulet, P. (1994). Structure of the polyglutamyl chain of tubulin: occurrence of alpha and gamma linkages between glutamyl units revealed by monoreactive polyclonal antibodies. *Biol. Cell* **81**, 11-16.

Young, A., Dictenberg, J. B., Purohit, A., Tuft, R. and Doxsey, S. J. (2000). Cytoplasmic dynein-mediated assembly of pericentrin and gamma tubulin onto centrosomes. *Mol. Biol. Cell*. **11**, 2047-2056.

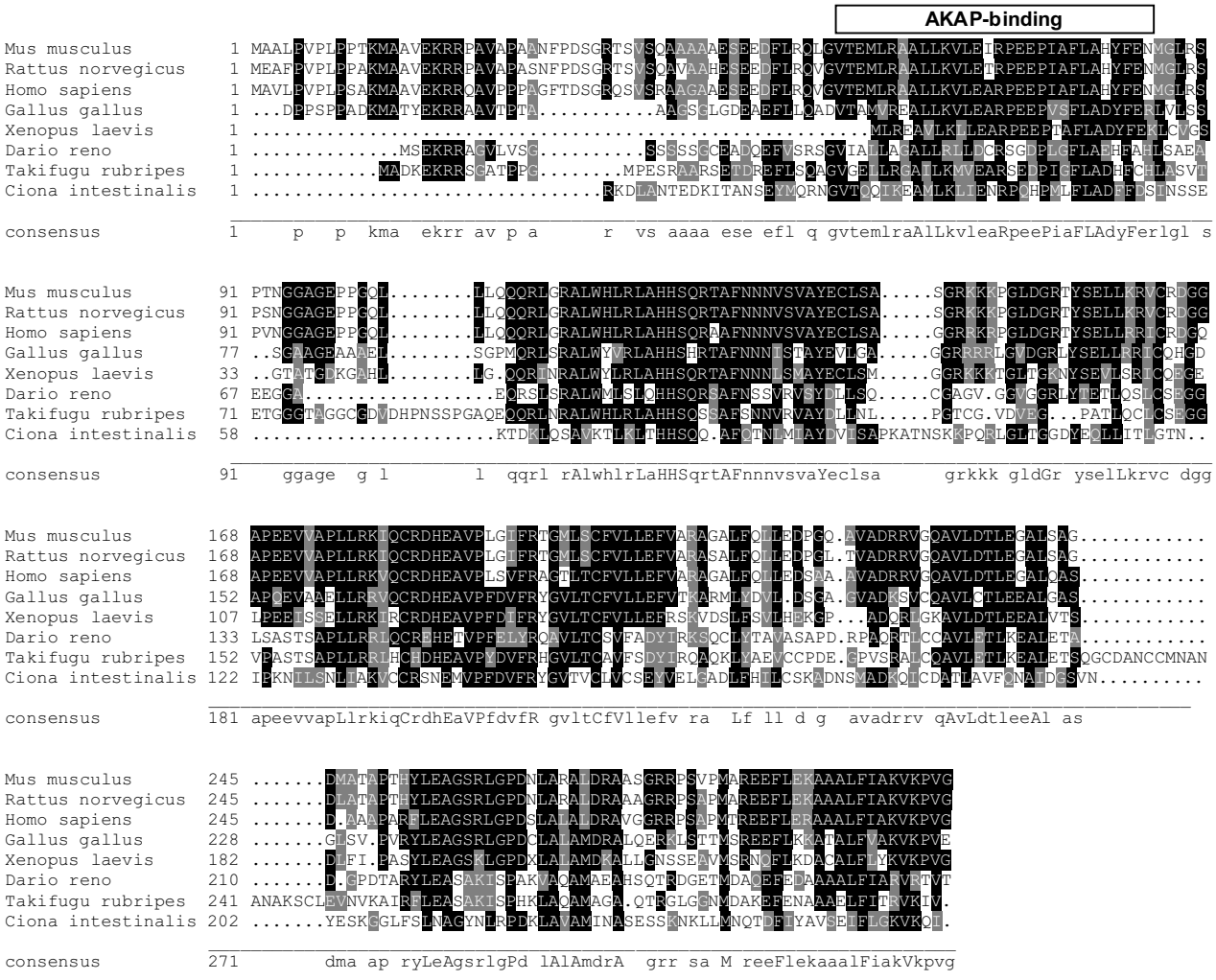

Supplementary figure 1: Alignment of potential homologues of PGs1. The alignment (Clustal method) of the protein sequences of potential homologues of PGs1 from different organisms is shown. Completely conserved amino acid residues are boxed black, similar residues are boxed grey. Full-length cDNA sequences were received from Genebank for *Mus musculus* (Q 99MS8), *Takifugu rubripes* (SINFRUP00000085201) and *Xenopus laevis* (BU899349). Partial cDNA or ESTs sequences with overlapping sequence regions were received for *Ciona intestinalis* (ESTs: rcign041g09 34-241, rcign041g09 134-302, rcicl103o10 149-302, cieg071i12 150-302, rcieg081d01 169-302, cieg075m07 176-302, cicl013c05 192-302), *Dario reno* (BI472637, AL906882, BI472379), *Gallus gallus* (603584642F1, 603583417F1), *Homo sapiens* (AAH09520, XP042012.1 (BC009520)) and *Rattus norvegicus* (BF420090, AI575988). The full-length cDNA sequences for the latter were reconstructed using the Clustal multiple alignment strategy. cDNA sequences were translated using the standard genetic code.

The potential AKAP-binding motif is outlined.